

This is an Open Access document downloaded from ORCA, Cardiff University's institutional repository: <https://orca.cardiff.ac.uk/id/eprint/130374/>

This is the author's version of a work that was submitted to / accepted for publication.

Citation for final published version:

Galstyan, Anzhela, Maurya, Yogesh Kumar, Zhylitskaya, Halina, Bae, Youn Jue, Wu, Yi-Lin, Wasielewski, Michael R., Lis, Tadeusz, Dobrindt, Ulrich and St?pie?, Marcin  
2020.  $\pi$ -Extended Donor–Acceptor Porphyrins and Metalloporphyrins for Antimicrobial Photodynamic Inactivation. *Chemistry - A European Journal* 26 (37), pp. 8262-8266. 10.1002/chem.201905372

Publishers page: <http://dx.doi.org/10.1002/chem.201905372>

Please note:

Changes made as a result of publishing processes such as copy-editing, formatting and page numbers may not be reflected in this version. For the definitive version of this publication, please refer to the published source. You are advised to consult the publisher's version if you wish to cite this paper.

This version is being made available in accordance with publisher policies. See <http://orca.cf.ac.uk/policies.html> for usage policies. Copyright and moral rights for publications made available in ORCA are retained by the copyright holders.



# $\pi$ -Extended Donor–Acceptor Porphyrins and Metalloporphyrins for Antimicrobial Photodynamic Inactivation

Anzhela Galstyan,<sup>\*[a]</sup> Yogesh Kumar Maurya,<sup>[b]</sup> Halina Zhylitskaya,<sup>[b]</sup> Youn Jue Bae,<sup>[c]</sup> Yi-Lin Wu,<sup>‡[c]</sup> Michael R. Wasielewski,<sup>\*[c]</sup> Tadeusz Lis,<sup>[b]</sup> Ulrich Dobrindt,<sup>[d]</sup> Marcin Stępień<sup>\*[b]</sup>

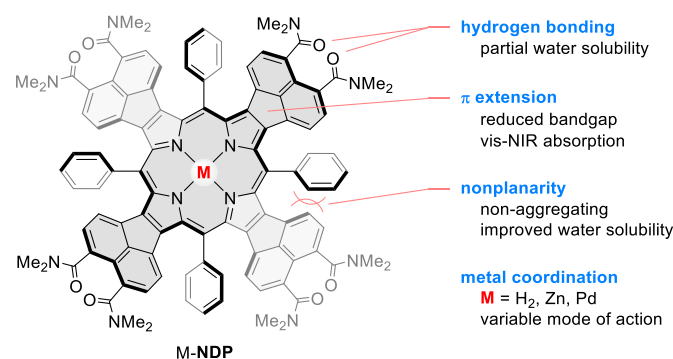
**Abstract:** Free base, zinc and palladium  $\pi$ -extended porphyrins containing fused naphthalenediamide units were employed as photosensitizers in antimicrobial photodynamic therapy (aPDT). Their efficacy, assessed by photophysical and *in vitro* photobiological studies on Gram-positive bacteria, was found to depend on metal coordination, showing a dramatic enhancement of photosensitizing activity for the palladium complex.

## Introduction

Multidrug resistance is a major reason for failure in the treatment of infections and thus antimicrobial strategies that do not contribute to the selection of pathogenic bacteria are currently gaining attraction.<sup>1</sup> In particular, antimicrobial photodynamic therapy (aPDT) has been proposed as an alternative approach for the treatment of bacterial infections.<sup>2</sup> In aPDT, reactive oxygen species (ROS) produced by an irradiated photosensitizer (PS) attack proteins, nucleic acids and lipids, causing bacterial cell death.<sup>3</sup> These ROS are generated either through electron or hydrogen transfer to substrates (type I mechanism) or by energy transfer to molecular oxygen with generation of singlet oxygen (<sup>1</sup>O<sub>2</sub>, type II mechanism).<sup>3c–e</sup>

Currently, porphyrin derivatives and their precursors are the most widely used PSs in clinics.<sup>4</sup> These include HpD (Photofrin<sup>®</sup>), Verteporfin (Visudyne<sup>®</sup>), *meso*-tetra(*m*-hydroxyphenyl)chlorin (Foscan<sup>®</sup>), lutetium texaphyrin (Antrin<sup>®</sup>), mono-L-aspartyl chlorin  $\epsilon_6$  (LS11), 2-(1-hexyloxyethyl)-2-divinyl

pyropheophorbide *a* (Photochlor), and 1,5-aminolevulinic acid and its derivatives as precursors of protoporphyrin IX (Levulan<sup>®</sup>, Metvix<sup>®</sup>).<sup>5</sup> Tetrapyrrole photosensitizers mostly exhibit type II activity, but their mode of action can be tuned by varying the substituents or the central metal atom.<sup>6</sup> Despite widespread clinical use, porphyrin-based systems have several drawbacks, in particular their relatively low absorptivity in the visible and near-infrared regions. Since longer absorption wavelengths are strongly preferred for *in vivo* applications, the porphyrin ring system has been variously modified to enhance absorption in the red and near-infrared regions. This effect can be achieved via partial  $\beta$ -hydrogenation, as in chlorins ( $\lambda_{\text{abs}}^{\text{max}} = 650$  nm) and bacteriochlorins ( $\lambda_{\text{abs}}^{\text{max}} = 780$  nm).<sup>7</sup> However, these derivatives are generally unstable and are readily oxidized back to the corresponding porphyrins upon irradiation. Alternatively, long-wavelength absorption can be enhanced by annulation of carbo- and heterocycles to the periphery of the porphyrin.<sup>8</sup> However, because of the more challenging synthesis and usually low solubility of the final products in aqueous media, the use of such  $\pi$ -extended porphyrins used in PDT remains limited.<sup>9</sup>



**Scheme 1.** Design principle of  $\pi$ -extended porphyrins used in this study.

Here we report on the use of  $\pi$ -extended porphyrins and metalloporphyrins as aPDT photosensitizers. The systems used in this study, labeled **M-NDP** (Scheme 1), contain four naphthalenediamide units fused to the  $\beta$ -pyrrolic positions of the porphyrin ring. We show that their activities against Gram-positive *Staphylococcus aureus* (*S. aureus*) 3150/12 and *Bacillus subtilis* (*B. subtilis*) DB104 are highly dependent on the metal coordination status of the porphyrin macrocycle ( $M = 2\text{H}$ , Zn and Pd).

- [a] A. Galstyan  
Center for Soft Nanoscience; Westfälische Wilhelms-Universität  
Münster. Busso-Peus-Straße 10, 48149 Münster, Germany.  
E-mail: anzhela.galstyan@wwu.de
- [b] Y. K. Maurya, H. Zhylitskaya, T. Lis, M. Stępień  
Wydział Chemii, Uniwersytet Wrocławski, ul. F. Joliot-Curie 14, 50-  
383 Wrocław, Poland.  
E-mail: marcin.stepien@chem.uni.wroc.pl
- [c] Y. J. Bae, Y.-L. Wu, M. R. Wasielewski  
Department of Chemistry and Institute for Sustainability and Energy  
at Northwestern, Northwestern University, Evanston, Illinois, 60208  
3113, United States  
E-mail: m-wasielewski@northwestern.edu  
‡ Current address: School of Chemistry, Cardiff University, Main  
Building, Park Place, Cardiff CF10 3AT, United Kingdom
- [d] U. Dobrindt  
Institute of Hygiene, Westfälische Wilhelms-Universität Münster,  
Mendelstraße 7, D-48149 Münster, Germany

Supporting information for this article is given via a link at the end of the document

## Results and Discussion

**H<sub>2</sub>-NDP**, obtained according to a recently reported procedure,<sup>10</sup> was transformed into its Zn and Pd complexes using established methods (Supporting Information). The steric congestion around the porphyrin core in **M-NDP**, caused by combined *meso*-substitution and  $\beta$ -fusion, results in a significant out-of-plane distortion of the aromatic surface, clearly seen in the solid-state geometry of **Pd-NDP** (Figure 1). The dimethylaminocarbonyl substituents are twisted relative to the peripheral naphthalene units, producing additional steric bulk that precludes direct  $\pi$ - $\pi$ -stacking interactions between molecules. As a consequence, **H<sub>2</sub>-NDP** and **Pd-NDP** do not aggregate significantly in organic solvents, as evidenced by their concentration-independent optical absorption spectra. **Zn-NDP** was previously found to undergo specific aggregation in chloroform solutions,<sup>10</sup> which was attributed to intermolecular coordination of amide substituents to Zn centers in **Zn-NDP**. The latter effect was however observed at relatively high concentrations (ca.  $10^{-2}$  to  $10^{-3}$  M) and it appears to have no significant influence on the absorption spectra of **Zn-NDP** recorded for more dilute samples ( $10^{-5}$  to  $10^{-6}$  M, Figure S5, Supporting Information). While DLS data obtained in water (Figure S9, Supporting Information) indicate the formation of nanoparticles, absorption spectra of **NDPs** remain concentration-independent in the  $10^{-5}$  to  $10^{-6}$  M range (Figure S6, Supporting Information), and resemble those observed in DCM solutions.

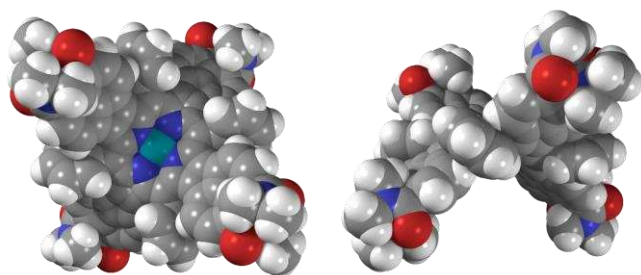


**Figure 1.** Molecular geometry of **Pd-NDP**, obtained from an X-ray crystallographic analysis, showing the deep saddle distortion of the chromophore.

Photophysical properties were initially measured in dichloromethane (DCM) to assess the PS performance (Figure 2 and Table 1). All **NDP** photosensitizers showed absorption bands extending from 300 to 700 nm, presenting multiple opportunities for electronic excitation in close proximity to the near-infrared spectral range. The most intense absorption maxima of the **M-NDP** dyes appear at 541–573 nm and are bathochromically shifted relative to the Soret bands of hematoporphyrin (395 nm) and protoporphyrin IX (398 nm) in DCM, consistent with the expanded  $\pi$ -conjugation of the **NDP** chromophore. Molar extinction coefficients of the largest peaks ( $> 10^5$  L mol<sup>-1</sup> cm<sup>-1</sup>, Table S2, in the Supporting Information) are comparable for all derivatives and consistent with the previous report. As observed previously for other palladium(II) porphyrins,

the Soret and Q bands of **Pd-NDP** are blue-shifted in comparison with **Zn-NDP** and **H<sub>2</sub>-NDP**, with a characteristic intensity increase of the Q(1,0) transition.<sup>11</sup> This observed trend is semi-quantitatively reproduced by time-dependent density functional theory (TD-DFT) calculations which reveal a larger optical band gap in the **Pd-NDP** system relative to the **Zn-NDP** and **H<sub>2</sub>-NDP** chromophores (Supporting Information), in line with the experiment. This change is mostly attributed to the lower energy of the HOMO level in the **Pd-NDP** complex (Supporting Information).

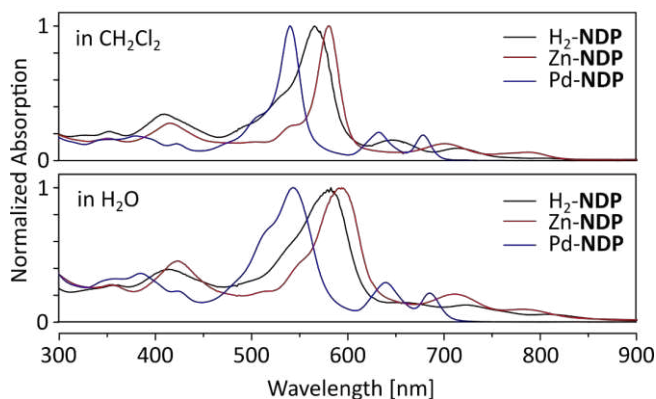


**Figure 2.** Optical absorbance of **H<sub>2</sub>-NDP** (black), **Zn-NDP** (red) and **Pd-NDP** (blue) in DCM (top) and H<sub>2</sub>O (bottom). Molar concentrations were  $1 \times 10^{-5}$  M.

Importantly for their prospective application as PSs, each of the three **M-NDP** derivatives could be solubilized in water (containing less than 1% DMSO), at practically useful concentrations (ca.  $10^{-5}$  M). This solubility enhancement, which is also reflected in the  $\log P_{o/w}$  values (Table 1), is caused by the combination of amide substitution and non-planarity of the **NDP** chromophore. **Pd-NDP** is the least soluble in water among the three derivatives. In aqueous media, absorption bands of the **M-NDP** systems are broadened and red-shifted. This effect is more pronounced for **H<sub>2</sub>-NDP** and **Zn-NDP** (17 and 18 nm, respectively, for the Soret band) and is apparently consistent with the positive solvatochromism observed for related donor-acceptor oligopyrroles.<sup>12</sup> The absorptivity of **Pd-NDP** in water is significantly lower than measured for **H<sub>2</sub>-NDP** and **Zn-NDP**, possibly indicating a more aggregated state of **Pd-NDP** in this solvent. All **M-NDP** derivatives display negligible fluorescence in solution ( $\Phi_{fl} \ll 1\%$ ), suggesting an excited-state decay pathway competitive to singlet emission, caused by the non-planar structures of these  $\pi$ -extended chromophores (see below).

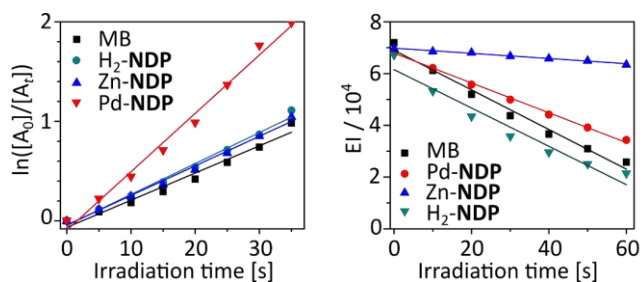


**Figure 3.** (a) The plot of DPBF absorbance change and (b) ABMDMA emission change as a function of irradiation time. DPBF, 1,3-diphenylisobenzofuran; ABMDMA, 9,10-anthracenediyl-bis(methylene)dimalonic acid; EI, emission intensity integral.

Excited-state lifetimes of the three PSs were measured in deoxygenated dichloromethane using transient absorption spectroscopy (Table 1 and Supporting Information). As suggested by the  $\mu\text{s}$  lifetimes, all three **NDP** derivatives form triplets, likely through the spin-orbit coupling mechanism. In the case of Pd-**NDP**, the heavy-metal effect enhances intersystem crossing as shown in the shorter triplet formation time constant,  $\tau_{\text{S}\rightarrow\text{T}}$ . In addition,  $\tau_{\text{S}\rightarrow\text{T}}$  for H<sub>2</sub>-**NDP** and Zn-**NDP** ( $605 \pm 2$  and  $530 \pm 10$  ps respectively), are reduced relative to the value determined for zinc(II) *meso*-tetraphenylporphyrin (Zn**TPP**,  $\sim 2000$  ps in toluene),<sup>13</sup> and compare well with the time constant reported for zinc(II) *meso*-tetraphenyltetrabenzoporphyrin (Zn**TBTPP**,  $291 \pm 7$  ps in toluene).<sup>14</sup> In the case of Zn**TBTPP** and M-**NDPs**, the saddle distortion of the chromophore may be a major source of spin-orbit coupling.<sup>15</sup> This rapid triplet formation accounts for the observed low fluorescence and suggests applicability of **NDP** dyes for oxygen sensitization.

**Table 1.** Photophysical data for H<sub>2</sub>-**NDP**, Zn-**NDP**, and Pd-**NDP**.

PS	$\log P_{\text{ow}}^{[a]}$	$\Phi_{\Delta}^{[b]}$ (DCM)	$\Phi_{\Delta}^{[b]}$ (H <sub>2</sub> O)	Triplet states <sup>[c]</sup>		
				$\lambda_{\text{ex}}$ nm	$\tau_{\text{S}\rightarrow\text{T}}^{[d]}$ ps	$\tau_{\text{T}\rightarrow\text{GS}}^{[e]}$ $\mu\text{s}$
H <sub>2</sub> - <b>NDP</b>	0.31	0.59	0.50	600	$605 \pm 2$	$54 \pm 1$ $210 \pm 10$
Zn- <b>NDP</b>	0.32	0.57	0.07	580	$530 \pm 10$	$77 \pm 1$ $250 \pm 10$
Pd- <b>NDP</b>	0.51	1.00	0.39	540	$2.6 \pm 0.1$	$20 \pm 1$ $52 \pm 3$

[a] 1-Octanol/water partition coefficient. [b] Quantum yields of singlet oxygen photogeneration measured using the relative method and methylene blue as a reference. Estimated accuracy  $\pm 0.03$ . [c] Triplet formation and decay (deoxygenated dichloromethane, excitation at  $\lambda_{\text{ex}}$ ). [d] Singlet (S) to triplet (T) intersystem crossing. [e] Decay of triplet (T) to the ground state (GS); the observed biexponential decay may be related to (i) collisional triplet-triplet annihilation and/or (ii) aggregation/conformation changes (see the Supporting Information for additional discussion).

Irreversible photooxidation of 1,3-diphenylisobenzofuran (DPBF), a non-selective probe for singlet oxygen and reactive oxygen species, was used to evaluate the ability of the M-**NDP**

dyes to generate ROS in DCM. In these experiments, methylene blue (MB), was used as the reference. Upon irradiation with visible light (xenon lamp,  $5 \text{ mW/cm}^2$ ,  $\lambda > 515 \text{ nm}$ ), all M-**NDP** porphyrins produced significant decay of the DPBF absorption, monitored at 414 nm. The quantum yield of singlet oxygen photogeneration of Pd-**NDP** in DCM (Table 1) was higher than the values determined for Zn-**NDP** and H<sub>2</sub>-**NDP**, reflecting the heavy atom effect of Pd, which increases the yield of intersystem crossing from the excited singlet to lowest energy triplet excited state. A quantitative analysis of photooxidation reactions leading to the loss of emission (409 and 431nm) of the water-soluble anthracene 9,10-dipropionic acid (ABMDMA) was used to measure <sup>1</sup>O<sub>2</sub> production in aqueous media. In contrast to the measurements in DCM, Pd-**NDP** and H<sub>2</sub>-**NDP** exhibit greater singlet oxygen quantum yields in comparison with Zn-**NDP**.

Since the M-**NDP** photosensitizers are not positively charged, they are most suitable to target Gram-positive bacteria.<sup>16</sup> We choose two representative strains *S. aureus* 3150/12 and *B. subtilis* DB104 to study antibacterial activity of M-**NDPs**. Pathogens such as *S. aureus* are one of the major causes of community and hospital-acquired infections, with significant morbidity and mortality. The non-pathogenic *B. subtilis* is a normal gut commensal in humans and is considered the best studied Gram-positive bacterium. Killing assays were performed after incubation of ca.  $10^8$  colony-forming unit/mL (CFU/mL) with  $10 \mu\text{M}$  of the corresponding M-**NDP** for 15 min and plating aliquots after a certain time of irradiation (30, 60 and 90 min) with light passing through a 515 nm cut-off filter. The results of the determination of antibacterial effect are summarized in Figure 4.

Under identical conditions, the viability of both strains showed significant dependence on the porphyrin derivative used. Pd-**NDP** was found out to be more potent against both tested bacteria with different inactivation kinetics. For instance, no colony was found on the agar plate when *S. aureus* 3150/12 was treated with Pd-**NDP** and irradiated for 60 min ( $18 \text{ J/cm}^2$ ). This was not the case when *B. subtilis* DB104 was used. Nevertheless bactericidal effect ( $> 3 \log_{10}$  steps reduction) and disinfecting effect ( $> 5 \log_{10}$  steps reduction) could be achieved after 60 min and 90 min irradiation, correspondingly. H<sub>2</sub>-**NDP** and Zn-**NDP** showed to be less active with both bacterial strains. However, when treated with H<sub>2</sub>-**NDP** and light (90 min,  $27 \text{ J/cm}^2$ ), the reduction in  $\log_{10}$  unit was 3.15 for *S. aureus* 3150/12 and 4.47 for *B. Subtilis* DB104, respectively. Under identical irradiation conditions Zn-**NDP** effected a reduction of less than 3  $\log_{10}$  units. Visual inspection of the fluorescence images of Live/Dead stained *S. aureus* 3150/12 after incubation with M-**NDPs** and irradiation with  $9 \text{ J}\cdot\text{cm}^{-2}$  light doses further confirmed the activity of Pd-**NDP** (Figure S18, Supporting Information). Numerous viable microorganisms (green fluorescence) were visible in the control sample and in the samples of *S. aureus* 3150/12 treated with H<sub>2</sub>-**NDP** and Zn-**NDP**. In contrast, a large number of dead bacterial cells (red fluorescence) appeared when Pd-**NDP** was used. The fluorescence images of *B. subtilis* DB104 treated with M-**NDP** and irradiated under similar

conditions showed mostly viable bacteria, consistent with the results of CFU counting.

The markedly lower photocytotoxicities of H<sub>2</sub>-NDP and Zn-NDP compared to Pd-NDP suggest that important intracellular targets are damaged more efficiently when Pd-NDP was used. Commonly, molecular characteristics such as the targeting unit, charge, asymmetry and lipophilicity govern binding and uptake of the PS into bacterial cells.<sup>17</sup> Although we used a homologous set of porphyrins, Pd-NDP has a higher log *P*<sub>0/w</sub> value, which could contribute to improved cellular uptake and efficient

damage of the bacterial cell. ROS quantum yields determined in aqueous media do not appear to be sufficient to explain the observed differences in phototoxicity. Literature reports describe that the palladium bacteriochlorin sensitizer **TOOKAD** can produce different reactive oxygen species in different environments.<sup>18</sup> Thus, to investigate the underlying mechanism of the bacterial inactivation and find out whether aPDT efficacy is affected by the nature and persistence of the ROS two different quenchers, sodium azide and mannitol, were used in irradiation experiments.<sup>19</sup>

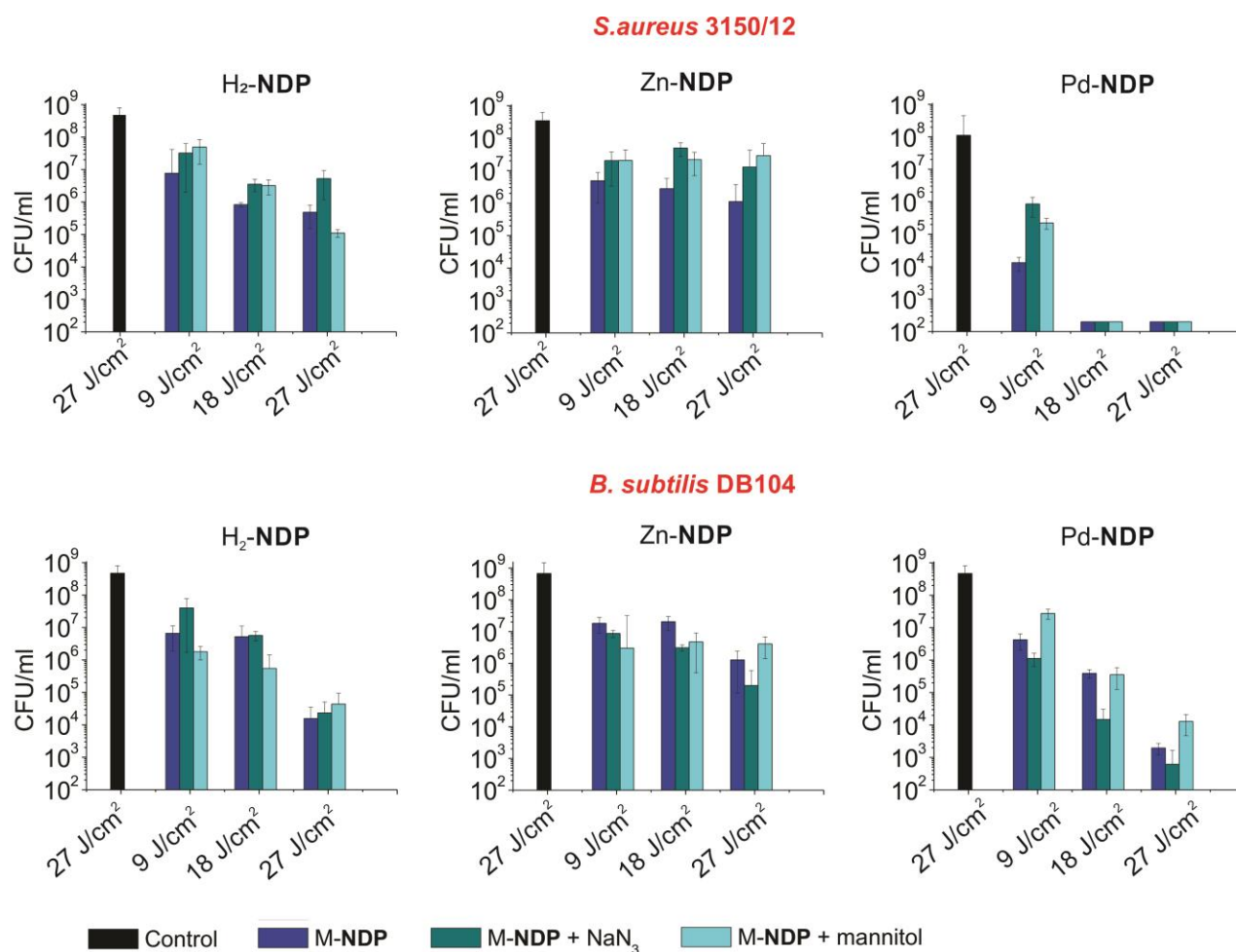


**Figure 4.** Histograms showing the photodynamic inactivation of *S. aureus* 3150/12 and *B. Subtilis* DB104 in planktonic cultures treated with H<sub>2</sub>-NDP, Zn-NDP, and Pd-NDP. Control group are bacteria without any treatment. Irradiation conditions:  $\lambda > 515$  nm, 5 W cm<sup>-2</sup>, 30, 60 and 90 min. The concentration of PSs is 10  $\mu$ M.

Although neither of these two scavengers could provide complete protection from inactivation, both sodium azide and mannitol had an effect on the viability of microorganisms. Comparison of the photodynamic effect of Pd-NDP for *S. aureus* 3150/12 and *B. subtilis* DB104 in the presence of sodium azide showed that the mode of action of Pd-NDP is most likely different for these two strains. Whereas for *S. aureus* 3150/12 photocytotoxicity was reduced indicating that killing of bacteria was mainly due to the generation of <sup>1</sup>O<sub>2</sub> via type II mechanism,

for *B. subtilis* DB104 potentiation of the aPDT effect was observed. Mannitol, which is known to quench hydroxyl radicals formed in the type I mechanism, was found to reduce the activity of Pd-NDP against both bacterial strains. These results suggest that the photosensitization by Pd-NDP is based on a combination of type I and type II mechanisms. For H<sub>2</sub>-NDP and Zn-NDP this effect was not pronounced. A strain-dependent photochemical mechanism was previously reported by Hamblin et al. for a homologous series of phenothiazinium dyes.<sup>20</sup> The

mechanism of action was proposed to depend on the microenvironment, e.g. higher binding of the dye to bacteria. In another study based on series of meso-tetraarylporphyrins, Almeida et al. showed for the series of PSs that the mechanism of action of the certain PS depends on structure (number and placement of charges), aggregation behavior, and affinity for the cell membrane t.<sup>21</sup>

## Conclusions

In summary,  $\pi$ -extended porphyrins containing peripheral naphthalenediamide subunits are examined here as aPDT photosensitizers for the first time. These systems feature intense vis-NIR absorption, sufficient solubility in water, achieved without additional functionalization, and appreciable quantum yields of singlet oxygen photogeneration. The aPDT efficiency of M-NDP photosensitizers can be tuned by metal coordination, showing that this family of dyes could be used for treatment of infections caused by Gram-positive bacteria. The photosensitizing potential of other donor-acceptor oligopyrrole chromophores is currently explored in our laboratories.

## Experimental Section

For full details, please see the Supporting Information.

## Acknowledgements

This work was supported by the Foundation for Polish Science (TEAM POIR.04.04.00-00-5BF1/17-00, to MS), U.S. Department of Energy, Office of Science, Office of Basic Energy Sciences under Award DE-FG02-99ER14999 (MRW), German Research Foundation (DFG GA 2362/2-1, to AG), and Fonds der Chemischen Industrie (to AG).

## Conflict of Interest

The authors declare no conflict of interest.

**Keywords:**  $\pi$ -extended porphyrins • antimicrobial • triplet state • singlet oxygen • photosensitizers

- [1] (a) A. Gupta, R. F. Landis, C.-H. Li, M. Schnurr, R. Das, Y.-W. Lee, M. Yazdani, Y. Liu, A. Kozlova, V. M. Rotello, *J. Am. Chem. Soc.* **2018**, *140*, 12137-12143; (b) P. R. Judzewitsch, T.-K. Nguyen, S. Shanmugam, E. H. H. Wong, C. Boyer, *Angew. Chem. Int. Ed.* **2018**, *57*, 4559-4564; (c) J. D. Steckbeck, B. Deslouches, R. C. Montelaro, *Expert. Opin. Biol. Ther.* **2014**, *14*, 11-14; (d) C. D. Fjell, J. A. Hiss, R. E. W. Hancock, G. Schneider, *Nat. Rev. Drug Discov.* **2012**, *11*, 37-51.
- [2] (a) A. Regiel-Futyra, J. M. Dąbrowski, O. Mazuryk, K. Śpiewak, A. Kyzioł, B. Pucelik, M. Brindell, G. Stochel, *Coord. Chem. Rev.* **2017**, *351*, 76-117; (b) Y. Liu, R. Qin, S. A. J. Zaat, E. Breukink, M. Heger, *J. Clin. Transl. Res.* **2015**, *1*, 140-167; (c) A. Galstyan, R. Schiller, U. Dobrindt, *Angew. Chem. Int. Ed.* **2017**, *56*, 10362-10366; (d) A. Galstyan, D. Block, S. Niemann, M. C. Grüner, S. Abbruzzetti, M. Oneto, C. G. Daniliuc, S. Hermann, C. Viappiani, M. Schäfers, B. Löffler, C. A. Strasser, A. Faust, *Chem. Eur. J.* **2016**, *22*, 5243-5252. (e) M. Wainwright, T. Maisch, S. Nonell, K. Plaetzer, A. Almeida, G. P. Tegos, M. R. Hamblin, *Lancet Infect. Dis.* **2017**, *17*, e49-e55.
- [3] (a) L. M. Mink, M. L. Neitzel, L. M. Bellomy, R. E. Falvo, R. K. Boggess, B. T. Trainum, P. Yeaman, *Polyhedron* **1997**, *16*, 2809-2817; (b) O. E. Akilov, K. O'Riordan, S. Kosaka, T. Hasan, *Med. Laser Appl.* **2006**, *21*, 251-260; (c) H. Horiuchi, A. Sakai, S. Akiyama, R. Ikeda, S. Ito, M. Furuya, Y. Gomibuchi, M. Ichikawa, T. Yoshihara, S. Tobita, T. Okutsu, *J. Photochem. Photobiol. A Chem.* **2017**, *339*, 19-24; (d) J.-Y. Zeng, M.-Z. Zou, M. Zhang, X.-S. Wang, X. Zeng, H. Cong, X.-Z. Zhang, *ACS Nano* **2018**, *12*, 4630-4640; (e) S. Callaghan, M. O. Senge, *Photochem. Photobiol. Sci.* **2018**, *17*, 1490-1514.
- [4] (a) E. S. Nyman, P. H. Hynninen, *J. Photochem. Photobiol. B* **2004**, *73*, 1-28. (b) E. Paszko, C. Ehrhardt, M. O. Senge, D. P. Kelleher, J. V. Reynolds, *Photodiag. Photodyn. Ther.* **2011**, *8*, 14-29. (c) V. Almeida-Marrero, E. van de Winkel, E. Anaya-Plaza, T. Torres, A. de la Escosura, *Chem. Soc. Rev.* **2018**, *47*, 7369-7400.
- [5] (a) S. Pushpan, S. Venkatraman, V. Anand, J. Sankar, D. Parmeswaran, S. Ganesan, T. Chandrashekar, *Curr. Med. Chem.* **2002**, *2*, 187-207; (b) J. Kou, D. Dou, L. Yang, *Oncotarget* **2017**, *8*.
- [6] (a) P. Mroz, J. Bhaumik, D. K. Dogutan, Z. Aly, Z. Kamal, L. Khalid, H. L. Kee, D. F. Bocian, D. Holten, J. S. Lindsey, M. R. Hamblin, *Cancer Lett.* **2009**, *282*, 63-76; (b) H. L. Kee, J. Bhaumik, J. R. Diers, P. Mroz, M. R. Hamblin, D. F. Bocian, J. S. Lindsey, D. Holten, *J. Photochem. Photobiol. A Chem.* **2008**, *200*, 346-355.
- [7] (a) S. Schastak, S. Ziganshyna, B. Gitter, P. Wiedemann, T. Claudepierre, *PLoS ONE* **2010**, *5*, e11674; (b) L. Huang, Y.-Y. Huang, P. Mroz, G. P. Tegos, T. Zhiyentayev, S. K. Sharma, Z. Lu, T. Balasubramanian, M. Krayner, C. Ruzie, E. Yang, H. L. Kee, C. Kirmaier, J. R. Diers, D. F. Bocian, D. Holten, J. S. Lindsey, M. R. Hamblin, *Antimicrob. Agents Chemother.* **2010**, *54*, 3834-3841.
- [8] (a) A. Tsuda, *Science* **2001**, *293*, 79-82; (b) T. Tanaka, A. Osuka, *Chem. Soc. Rev.* **2015**, *44*, 943-969; (c) J. Mack, Y. Asano, N. Kobayashi, M. J. Stillman, *J. Am. Chem. Soc.* **2005**, *127*, 17697-17711; (d) J. Mack, *Chem. Rev.* **2017**, *117*, 3444-3478; (e) Y. Saegusa, T. Ishizuka, K. Komamura, S. Shimizu, H. Kotani, N. Kobayashi, T. Kojima, *Phys. Chem. Chem. Phys.* **2015**, *17*, 15001-15011; (f) H.-J. Xu, J. Mack, D. Wu, Z.-L. Xue, A. B. Descalzo, K. Rurack, N. Kobayashi, Z. Shen, *Chem. Eur. J.* **2012**, *18*, 16844-16867; (g) C. Preihs, J. F. Arambula, D. Magda, H. Jeong, D. Yoo, J. Cheon, Z. H. Siddik, J. L. Sessler, *Inorg. Chem.* **2013**, *52*, 12184-12192.
- [9] (a) J. R. Sommer, A. H. Shelton, A. Parthasarathy, I. Ghiviriga, J. R. Reynolds, K. S. Schanze, *Chem. Mater.* **2011**, *23*, 5296-5304; (b) C. M. B. Carvalho, T. J. Brocksom, K. T. de Oliveira, *Chem. Soc. Rev.* **2013**, *42*, 3302.
- [10] H. Zhylitskaya, J. Cybińska, P. Chmielewski, T. Lis, M. Stępień, *J. Am. Chem. Soc.* **2016**, *138*, 11390-11398.
- [11] P. J. Spellane, M. Gouterman, A. Antipas, S. Kim, Y. C. Liu, *Inorg. Chem.* **1980**, *19*, 386-391.
- [12] (a) M. Żyła-Karwowska, H. Zhylitskaya, J. Cybińska, T. Lis, P. J. Chmielewski, M. Stępień, *Angew. Chem. Int. Ed.* **2016**, *55*, 14658-14662; (b) M. Żyła-Karwowska, L. Moshniha, Y. Hong, H. Zhylitskaya, J. Cybińska, P. J. Chmielewski, T. Lis, D. Kim, M. Stępień, *Chem. Eur. J.* **2018**, *24*, 7525-7530; (c) M. Navakouski, H. Zhylitskaya, P. J. Chmielewski, T. Lis, J. Cybińska, M. Stępień, *Angew. Chem. Int. Ed.* **2019**, *58*, 4929-4933.
- [13] N. Banerji, S. V. Bhosale, I. Petkova, S. J. Langford, E. Vauthey, *Phys. Chem. Chem. Phys.* **2011**, *13*, 1019-1029.
- [14] V. V. Roznyatovskiy, R. Carmieli, S. M. Dyar, K. E. Brown, M. R. Wasielewski, *Angew. Chem. Int. Ed.* **2014**, *53*, 3457-3461.
- [15] G. G. Gurzadyan, T.-H. Tran-Thi, T. Gustavsson, *J. Chem. Phys.* **1998**, *108*, 385-388.

- 
- [16] (a) G. Jori, C. Fabris, M. Soncin, S. Ferro, O. Coppellotti, D. Dei, L. Fantetti, G. Chiti, G. Roncucci, *Lasers Surg. Med.* **2006**, *38*, 468–481. (b) Z. Malik, J. Hanania, Y. Nitzan, *J. Photochem. Photobiol. B.* **1990**, *5*, 281–93. (c) M. R. Hamblin, *J. Antimicrob. Chemother.* **2002**, *49*, 941–951. (d) M. A. Pereira, M. A. F. Faustino, J. P. C. Tomé, M. G. P. M. S. Neves, A. C. Tomé, J. A. S. Cavaleiro, Â. Cunha, A. Almeida, *Photochem. Photobiol. Sci.* **2014**, *13*, 680.
- [17] (a) A. Galstyan, J. Putze, U. Dobrindt, *Chem. Eur. J.* **2018**, *24*, 1178–1186; (b) A. Galstyan, U. Dobrindt, *J. Mater. Chem. B* **2018**, *6*, 4630–4637; (c) C. Zhou, G. W. N. Chia, J. C. S. Ho, T. Seviour, T. Sailov, B. Liedberg, S. Kjelleberg, J. Hinks, G. C. Bazan, *Angew. Chem. Int. Ed.* **2018**, *57*, 8069–8072.
- [18] Y. Vakrat-Haglilii, L. Weiner, V. Brumfeld, A. Brandis, Y. Salomon, B. McIlroy, B. C. Wilson, A. Pawlak, M. Rozanowska, T. Sarna, A. Scherz, *J. Am. Chem. Soc.* **2005**, *127*, 6487–6497.
- [19] A. Tavares, S. R. S. Dias, C. M. B. Carvalho, M. A. F. Faustino, J. P. C. Tomé, M. G. P. M. S. Neves, A. C. Tomé, J. A. S. Cavaleiro, Â. Cunha, N. C. M. Gomes, et al., *Photochem. Photobiol. Sci.* **2011**, *10*, 1659–1669.
- [20] K. R. Kasimova, M. Sadasivam, G. Landi, T. Sarna, M. R. Hamblin, *Photochem. Photobiol. Sci.* **2014**, *13*, 1541–1548.
- [21] C. Vieira, A. T. P. C. Gomes, M. Q. Mesquita, N. M. M. Moura, M. G. P. M. S. Neves, M. A. F. Faustino, A. Almeida, *Front. Microbiol.* **2018**, *9*, DOI 10.3389/fmicb.2018.02665.
-

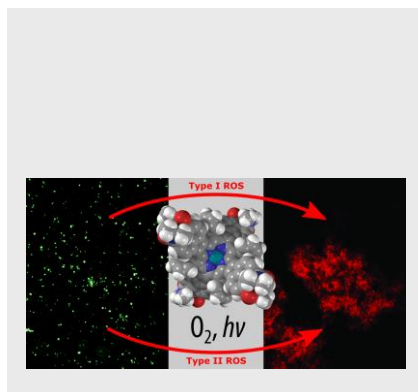
---

## Entry for the Table of Contents (Please choose one layout)

Layout 1:

---

Text for Table of Contents



Anzhela Galstyan,<sup>[a]</sup> Yogesh Kumar Maurya,<sup>[b]</sup> Halina Zhylitskaya,<sup>[b]</sup> Youn Jue Bae,<sup>[c]</sup> Yi-Lin Wu,<sup>‡[c]</sup> Michael R. Wasielewski,<sup>‡[c]</sup> Tadeusz Lis,<sup>[b]</sup> Ulrich Dobrindt,<sup>[d]</sup> Marcin Stępień<sup>‡[b]</sup>

**Page No. – Page No.**

**$\pi$ -Extended Donor–Acceptor Porphyrins and Metalloporphyrins for Antimicrobial Photodynamic Inactivation**

- 
- [a] A. Galstyan  
Center for Soft Nanoscience; Westfälische Wilhelms-Universität Münster. Busso-Peus-Straße 10, 48149 Münster, Germany.  
E-mail: anzhela.galstyan@wwu.de
- [b] Y. K. Maurya, H. Zhylitskaya, T. Lis, M. Stępień  
Wydział Chemii, Uniwersytet Wrocławski, ul. F. Joliot-Curie 14, 50-383 Wrocław, Poland.  
E-mail: marcin.stepien@chem.uni.wroc.pl
- [c] Y. J. Bae, Y.-L. Wu, M. R. Wasielewski  
Department of Chemistry and Institute for Sustainability and Energy at Northwestern, Northwestern University, Evanston, Illinois, 60208 3113, United States  
E-mail: m-wasielewski@northwestern.edu  
‡ Current address: School of Chemistry, Cardiff University, Main Building, Park Place, Cardiff CF10 3AT, United Kingdom
- [d] U. Dobrindt  
Institute of Hygiene, Westfälische Wilhelms-Universität Münster, Mendelstraße 7, D-48149 Münster, Germany

---

Supporting information for this article is given via a link at the end of the document. **((Please delete this text if not appropriate))**